Development of highly functional microfluidic devices for biochemical analyses

Graduate School of Pure and Applied Sciences

Development of highly functional microfluidic devices for biochemical analyses

（生化学分析のための高機能マイクロフルイディックデバイスの開発）

Shishir Kanti Pramanik

Doctoral Program in Nano-Science and Nano-Technology

Student ID No: 201630100

Doctor of Philosophy in Engineering

Advised by Prof. Hiroaki Suzuki

Summary

Chapter 1: Introduction

Many people suffer from infectious diseases in developing countries. However, traditional clinical diagnostic systems often work poorly in this context because they rely on expensive instruments usually set in central laboratories [1]. In this respect, point-of-care testing (POCT) is indispensable for prompt on-spot diagnosis and treatment of acute diseases by providing diagnostic results rapidly even by non-trained personnel [2]. For the development of diagnostic tools, the microfluidics technology has been spotlighted to meet the criterion of the POCT since they have remarkable features of high surface area to volume ratio resulting in fast diagnosis, reduced sample consumption, and a miniaturized format with portability and simplicity. The benefits of the microfluidic technology thus motive to have the widespread research determinations toward clinical diagnostic POCT for detecting numerous types of analytes [3].

Despite the significant progress in the field of detection and management of the infectious diseases, there are still many challenges for successful application of POCT microfluidic biochips as routine diagnostic devices, for example challenges with a good sensitivity, inexpensive manufacturing and affordable and compact signal detection. To address the current obstacle, it is desired to understand the fundamental aspects of microfluidic immunoassays and miniaturization including antibody immobilization, biological matrix interference, fluid control, surface passivation and signal detection modes. These multiple functions may be accomplished by integrating the indispensable components including microfluidic channel and active components such as valves, mixers, pumps and sensor [4]. However, immunoassays conducted with minimal external equipment's are mostly absent. Thus, there is of specific interest to develop inexpensive, portable immunoassay platform for POCT with minimum power consumption, with the reduction of components that are operated using external power sources.

For the successful application of POCT microfluidic diagnostic tools, the flow control in the integrated device with automatic or programmed operation presents a significant challenge. The fluid control is mostly performed by pumps and valves, which are operated by an external instruments set-up. Nowadays, an attempts have been considered to make the process automatic and simple for handling multiple reagents within a microchip. Devices with on-chip micropumps and microvalves were also used for this purpose [5, 6]. However, considering the use by non-professional end users, more simplified and reliable multiple solutions exchange is desired.

In this study, we introduce a microfluidic platform and methods to exchange of multiple solutions autonomously for biochemical analyses, especially for immunoassay purposes. First, an efficient exchange of multiple solutions was achieved by push-pull mechanism by creating a positive and negative pressure using a plastic syringe, and the usefulness of the device was demonstrated by conducting heterogonous immunoassay to detect human Interleukin 2 (IL-2). Later, the push-pull solutions exchange were realized on-chip more practically by integrating polymer-based micropumps.

Finally, we developed a new switchable hydrophobic valve and the integration of the valves into the integrated device facilitates the exchange of solutions efficiently on-chip with minimal user intervention.

Chapter 2: Valve-less microfluidic device with a push-pull sequential solution exchange function for fluorescence immunoassay

To detect proteins, enzyme-linked immunosorbent assay (ELISA) has been used widely [7]. However, conventional ELISA is labor intensive, consumes unnegligible volumes of expensive reagents, and requires a long assay time. In this respect, microfluidcs provides means for on-chip immunoassay. In realizing devices for POCT, a critical point is how

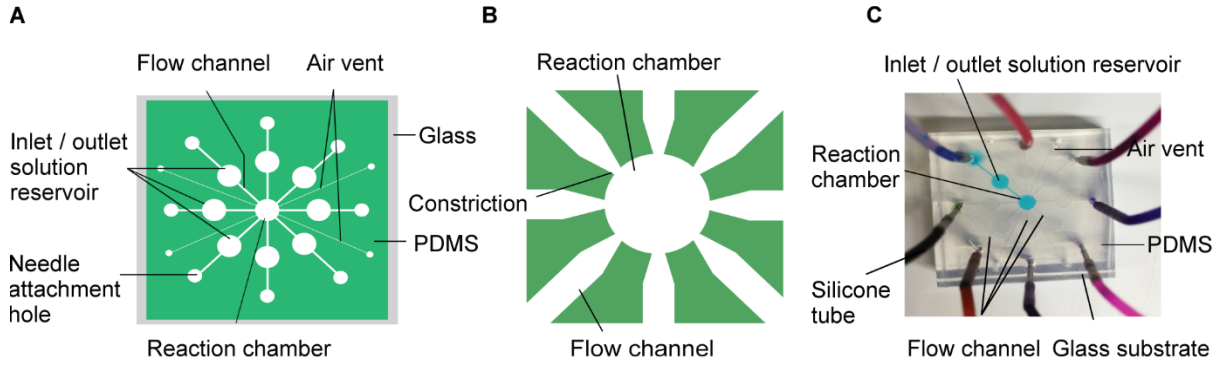

Figure 1. Microfluidic device for exchange of multiple solutions. (A) Top view. (B) Enlarge view of the device in which 50- μm constricted in the 200-μm flow channel at the entrance of the reaction chamber. (C) Photograph of the device with silicone tubes for injection of solutions and application of pressure.

to make the structure and procedure as simple as possible. In this study, we propose a novel method and device to realize an efficient solution exchange for biochemical analyses. In the exchange of solutions, a solution was introduced into a reaction chamber and was subsequently removed from there through the same flow channels one by one. To demonstrate the usefulness of this device, heterogonous immunoassay was conducted to detect human interleukin 2 (IL-2).

The device was constructed with glass and poly(dimethylsiloxane) (PDMS) substrates with a microfluidic structure. A reaction chamber, eight flow channels, solution reservoirs, and air vents were formed (Fig. 1). The structures were formed by replica molding using a mold formed with a thick-film photoresist SU-8 25 (MicroChem, Newton, MA, USA). The height of the flow channels and reaction chamber was 100 μm, and the diameter of the reaction chamber was 2 mm (volume: 310 nL). The flow channels were 200 μm wide, and the entrance of the flow channels to the reaction chamber was constricted to 50 μm to avoid entering of an injected solution into the other flow channels. The PDMS and glass substrates were bonded by oxygen plasma treatment for 15 s at 20 W and 25 Pa oxygen pressure.

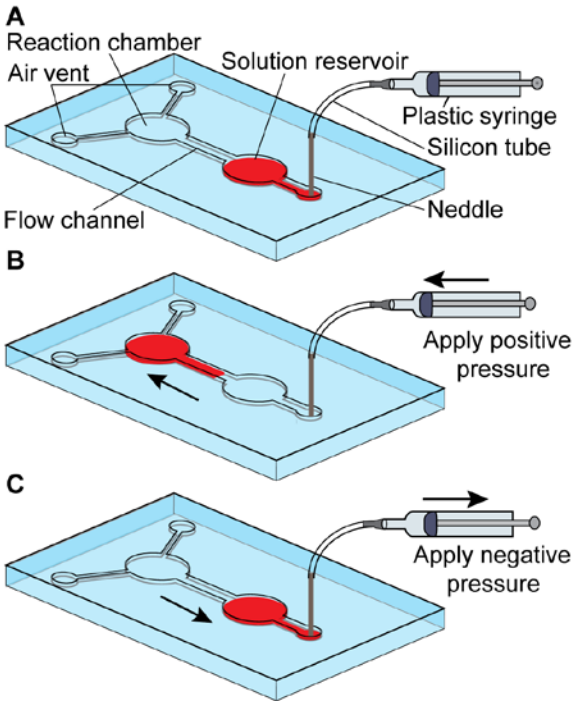

Figure 2. Solution exchange in the device. (A) Solution loaded. (B) Solution injected into the reaction chamber. (C) Solution removed from the reaction chamber.

Fig. 2 shows the procedure for the push-pull solution exchange. Silicone tubes were connected to plastic syringes and were filled with dye solutions. The other end of the

each tube was connected to the solution reservoirs of the chip. One of the solutions was injected into the reaction chamber by applying air pressure using the syringe. After the reaction chamber was completely filled with the solution, it was returned to the same solution reservoir by applying a negative pressure. The same steps were repeated for the other flow channels.

Fig. 3 shows the principle of detection of IL-2.To immobilize capture antibodies, solutions containing capture antibodies, APTES (3-Aminopropyl)triethoxysilane) (1% v/v), and coating buffer were introduced into the reaction chamber and incubated for 30 min at 4°C. Then, PBS (Phosphate-buffered saline) containing 0.5% BSA (Bovine serum albumin) and Tween 20 was introduced there and was incubated for 30 min to reduce non-specific binding of proteins. Then, to make the calibration curve, a series of IL-2 standard solutions containing IL-2 and FITC labeled detection antibodies were injected into the reaction chamber and were incubated for 25 min. After removing the solution, the reaction chamber was washed with PBS containing Tween 20, and fluorescence from the reaction chamber was detected using a fluorescence microscope (IX-73; Olympus, Japan).

Exchange of solutions was tested using devices with different flow channel widths (250 μm and 200 μm). While a solution was injected into the reaction chamber, the entire reaction chamber was filled with the solution. However, a part of the solution penetrated into the other flow channels. The most reproducible exchange of solutions was observed using the device with 200-μm wide flow channels and 50 μm constrictions at the reaction chamber (Fig. 1B). With this structure, solutions did not penetrate into the flow channels from the reaction chamber.

Fig. 4 shows how solutions were injected into the reaction chamber from different chambers and returned to each reservoir one by one. When the dye solutions were injected into the reaction chamber, the solutions did not enter the other flow channels. In addition, subsequent flushing of the solution via the same flow channel was performed very smoothly by applying a negative pressure. The solutions did not split during the process and no residues were left in the reaction chamber after flushing of the solutions. To examine the influence of hydrophobicity on solution exchange, the bottom of the reaction chamber was made hydrophobic by patterning a hydrophobic negative photo-resist OMR-83 (Tokyo Ohka Kogyo). No adverse influence was observed in solution exchange with the hydrophobic reaction chamber.

In order to demonstrate the usefulness of the device, fluorescence immunoassay was conducted to detect human IL-2. One of the flow channels was used for injecting and extracting

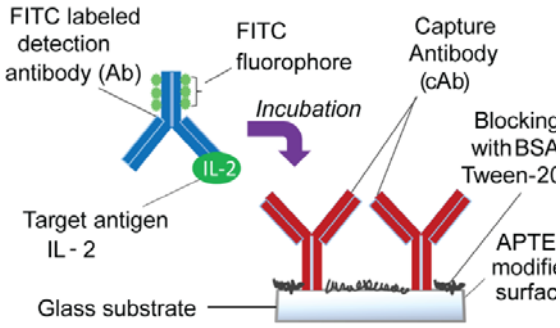

Figure 3. Principle of detection of IL-2 by sandwich fluorescence immunoassay.

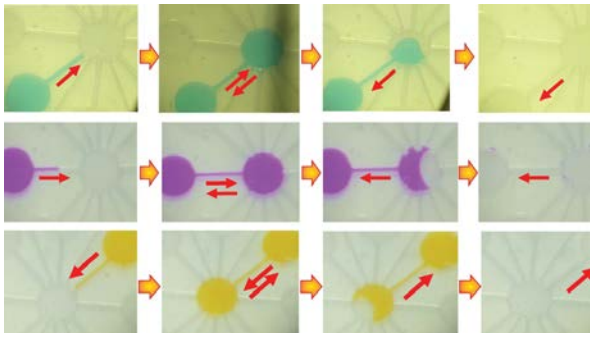

Figure 4. Images that show sequential exchange of solutions in the device.

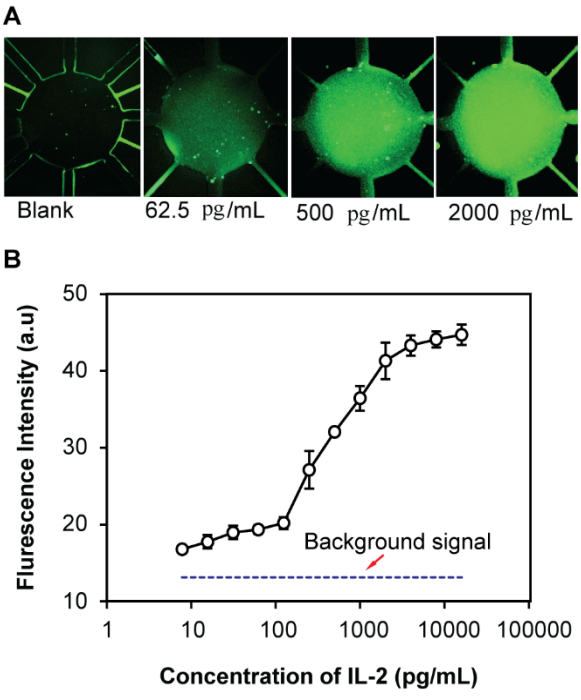

Figure 5. (A) Optical microscope images of fluorescence from the reaction chamber. (B) Dependence of fluorescence intensity on IL-2 concentration. Error bars represent means ± standard deviation for 3 replicates.

the mixture of coating buffer, 1 % (v/v) APTES, and capture antibodies (cAb). Two of the other flow channels were used to deliver a blocking reagent solution (0.5% BSA+ Tween 20) and a mixture of FITC labeled detection antibody and target antigen (IL-2), respectively. The other flow channels were used for washing.

Fig. 5A shows fluorescence from the reaction chamber. Fluorescence intensity depends on the number of IL-2 bound to the immobilized capture antibodies. Fig. 5B shows dependence of fluorescence intensity on IL-2 concentration. The fluorescence intensity increased with the increase in IL-2 concentration in a range of concentration between 125 pg/mL and 2.0 ng/mL. Weak fluorescence was observed from the reaction chamber even without IL-2, indicating the non-specific binding of dAb-FITC onto the surface. Fluorescence intensity tended to saturate at concentrations higher than 4 ng/mL. IL-2 could actually be detected within 25 min and the detection limit was 105 pg/mL.

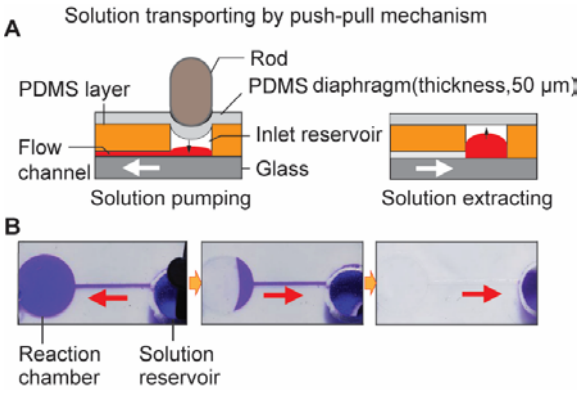

Figure 6. (A) Schematic illustration of the push-pull mechanism for injection and extraction of a solution in the reaction chamber by using elastic diaphragm and a small rod. (B) Photographs showing the movement of solution. The arrows indicate the direction of movement.

To transport solutions by the push-pull movement automatically, a 50 μm-thick elastic silicone rubber sheet was placed on solution reservoirs to form a diaphragm after solutions were introduced and was fixed. The Fig. 6 shows a preliminary experiment. Solutions in the reservoirs could be introduced into the reaction chamber by pushing the diaphragm. When the rod was removed, the elastic diaphragm recovered to the initial flat shape and the solutions were returned to the solution reservoir. The exchange of multiple solutions could be done efficiently one by one by rotating the device and push and release the diaphragm using a fixed rod.

Chapter 3: Polymer based on-chip micro-pump for exchanging of solutions in valve-less microfluidic device

Development of simple methods to transport of small volume solutions or reagents in a typical microfluidic platform is one of the key challenges for the successful application of the device for biochemical analyses [8]. Therefore, the chapter aims to develop a micropump that can be integrated into the microfluidic device for the efficient exchange of multiple solutions on-device. Specifically, the simple micropumps operated without external instruments will be used to realize automatic solution exchange in the developed immunoassay device. For this purpose, we present a superabsorbent polymer (SAP), sodium polyacrylate based micropump for solution injection into and extraction from the reaction chamber. When the polymer disc is in contact with water, the polymer absorbed large volume of water and the polymer network is expanded. Based on the swelling properties of the polymer, we designed sodium polyacrylate polymer actuated diaphragm micropump for solution injection from the inlet to the reaction chamber. On the other hand, for extraction of solution from the reaction chamber, we designed an extraction pump based on the superabsorbent properties of the polymer.

A superabsorbent cylindrical polymer discs were prepared by SP, CA and DI (deionized) water at an appropriate ratio (SP: 100 mg + CA:150 mg + 800 μL of H_2O). After that, thick semi-solid gel of the polymer containing inert supporting material (CA) was put into the PDMS template containing circular holes (diameter: 3.5 μm) that was formed by punching. Then, semi-solid gel in the template was kept at −80 °C for 2 h, followed by freeze drying at −50 °C for 3.5 h. After freeze-drying, the polymer discs were stored in air tight container to avoid the contact with the humid air.

The main structure and design of the device is illustrated in Fig. 7A. The device was constructed by bonding a glass substrate and four PDMS layers named bottom PDMS layer, diaphragm layer, PDMS actuation layer and PDMS top layer. Structure including flow channels, a reaction chamber (diameter: 2 mm), inlet solution reservoirs (diameter: 2 mm), the pump chambers were formed in the bottom PDMS layer by replica molding using a template made from the thick-film photoresist. Similarly, the PDMS actuation layer and PDMS top layer with the desire patterns were formed.

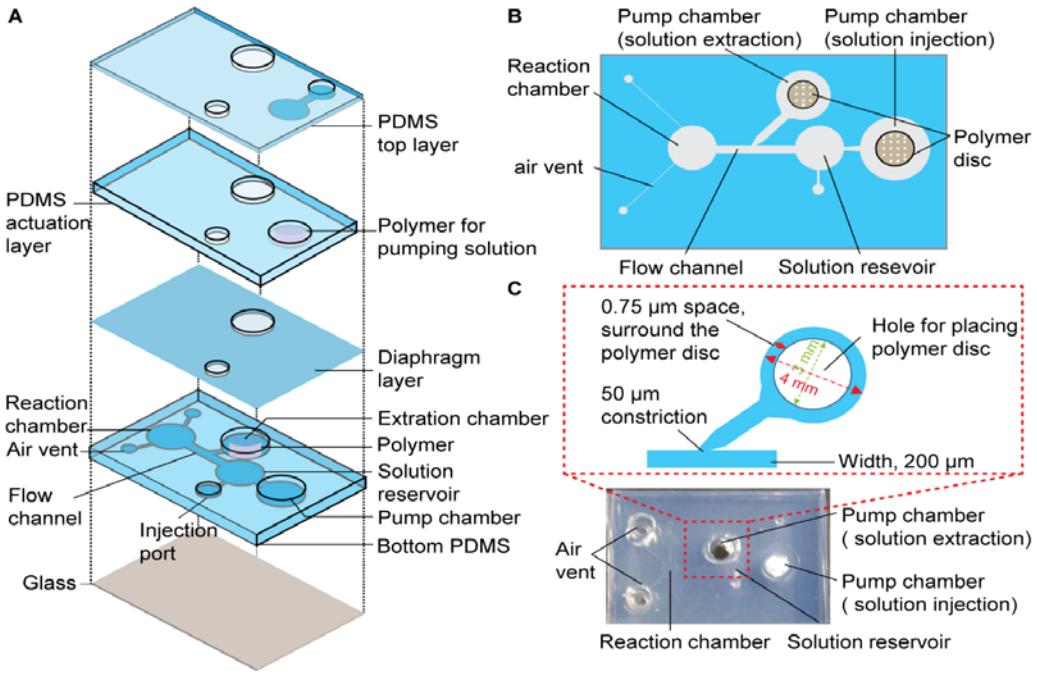

Figure 7. (A) Structure and design of the device with single flow channel for solution injection and extraction using the SP polymer disc. (B) Top view of the device (C) Photo of the compact device and structure of the extraction chamber along with its flow channel.

To fabricate 50-µm thick silicone rubber diaphragm, the PDMS prepolymer solution containing curing agent was spin-coated on the glass substrate at 1500 rpm for 10 min (3x), and then cured at 80 °C for 30 min. The circular shaped pump chamber with diameter 4.5 mm (for solution injection) was formed to one end of the main flow channel by punching holes (punch no. 1256, Takashiba Gimune Seisakujo, Hyogo, Japan) in the PDMS bottom layer. In the same manner, another circular shape compartment with a diameter 4 mm (for solution extraction) was formed between the reaction chamber and solution reservoir, and the compartment was connected to main flow channel through connecting flow channel at 45 degree angle (Fig 7C). In the PDMS actuation layer (PDMS 3rd layer), circular shape through-hole (4 mm) was formed for the insertion of the cylindrical polymer disc. In the top PDMS layer, a circular shape chamber (diameter: 4.5 mm) was connected to the inlet through the flow channel (1 mm long) that is designed to add priming solution to polymer disc for actuating the pump. In fabricating the final device, the device was assembled by layer by layer bonding of each layers by oxygen plasma treatment for 15 s at 20 W and 25 Pa oxygen pressure. The exchange of multiple solutions was achieved using a device with four flow channels and both pumps were connected to each flow channels.

Fig. 8 illustrates the working principle of the micropump. When small volume of DI water is added to the polymer disc, the volume changes of the polymer disc deflects the flexible PDMS diaphragm to the downward. As a result, the volume of a sealed pump chamber is decreased and thus generates a positive pressure to transport the solution (Fig. 8 ii). After completely full-filling the reaction chamber with the solution, the polymer disc was inserted into the extraction chamber. Once the solution is in contact with the disc, the solution started to move from reaction chamber to the extraction chamber (Fig. 8 iii, iv). The pump operation was video recorded using a microscope (Multiviewer system VB-S20, Keyence, Osaka, Japan).

The structure of the pump chamber for solution injection was optimized by measuring the injection flow rate using devices consisting with different cylindrical pump chambers of 7.0, 9.6, 12.5, 15.9 and 19.6 mm^2 and height of 2 mm. Distilled water containing food dye was used to measure the flow rate *Q*. Fig. 9 shows the relationship between the injection flow rates and different cross-sectional areas of the pump chamber. The flow rate increased linearly with the increase of cross sectional areas of the pump chamber. The highest flow rate was 25.8 µL/min and 26.2 µL/min for the

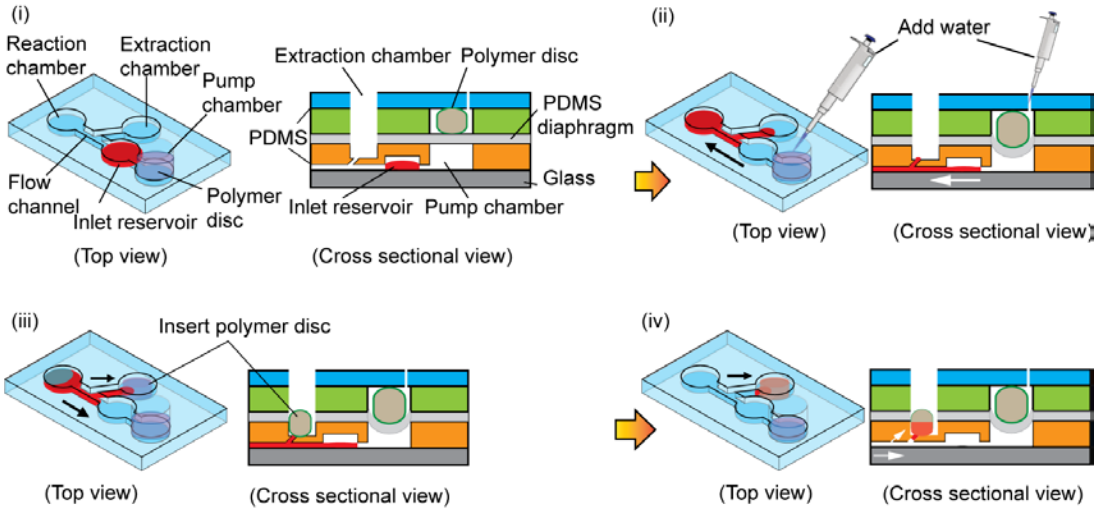

Figure 8. Working principle of the SP polymer actuated micropums for on- device solution exchange.

pump chamber of 15.9 and 19.6 mm^2, respectively. Furthermore, the chamber of the extraction pump was optimized by evaluating the entire solution extraction capability from the reaction chamber using the polymer disc while it was inserted into extraction chamber and the reaction chamber was completely filled with the injected solution. The devices designed with the extraction chamber of 4 mm in with a through hole of 3 mm in diameter offered the best performance with the entire solution extraction form the reaction chamber.

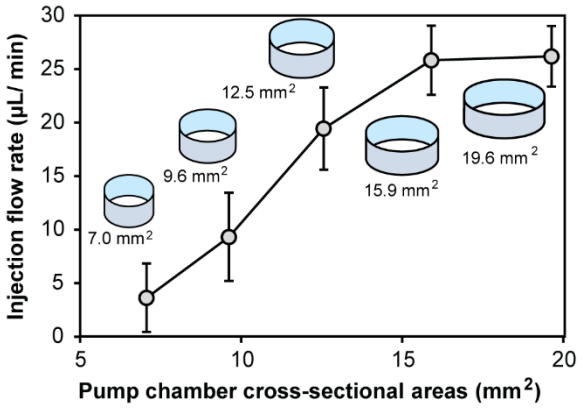

Figure 9. Injection flow rate of the SP polymer actuated pump at different cross-sectional area of the pump chamber. (n=3).

The performance of the pumps was characterized by checking the solution exchange capability of the pump. For this purpose, we measured the injection and extraction flow rate of aqueous sample solutions containing DI water, 0.1 M KCl, 0.1% (v/v), 1 M KCl, 0.1% (v/v), Glycerol (2X dilution) and Glycerol (99 %). Fig 10 shows the relationship between average flow rates (both injection and extraction flow rate) and sample solutions to be exchanged. The injection flow rate was almost identical (25.8 µL/min) for DI water, 0.1 M KCl and 1M KCl. However, the injection flow rate decreased to 17.4 and 2.7 µL/min for the viscous solutions of glycerol ((2x dilution) and glycerol (99%), respectively. In addition, the extraction flow rate decreased gradually for the solutions other than DI water (a constant flow rate: 0.73 µL/min). For the case of KCl solution, the low extraction flow rate is the result of the polyelectrolyte effect [9]. The extraction flow was observed substantial low for the Glycerol (2x dilution) solution, and for the case of glycerol (99%), solution was not extracted at all from the reaction chamber.

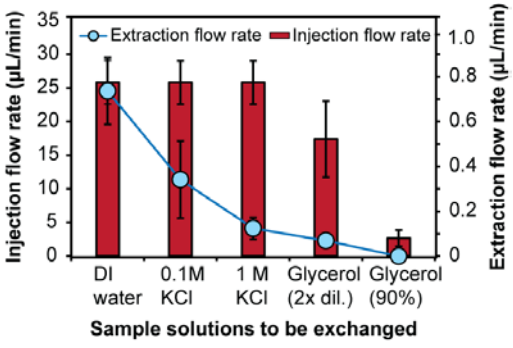

Figure 10. Injection and extraction flow rate as a function of sample solutions to be exchanged. n=6.

As the rate of swelling of polymer is decreased with the increasing of concentration of NaCl solution [10], we hypothesized that addition of the different concentrations of NaCl as a priming solution to the polymer disc would be influenced on the injection flow rate as well as the volume changes of the polymer disc. Our data confirmed this hypothesis. To control the injection flow rate, five concentration of NaCl solutions (0.5%, 1%, 2.5%, 5% and 10% aq. NaCl solution) and DI water containing no NaCl were used. Fig. 11 shows the dependence of the injection flow rate of DI water on DI water and different salt concentrations added to the polymer disc. The highest flow rate was obtained while DI water containing no NaCl was used, and the flow rate decreased gradually with the increases of NaCl concentration. For the case of addition of 10% NaCl solution, there was no solution flow from the inlet to the reaction chamber.

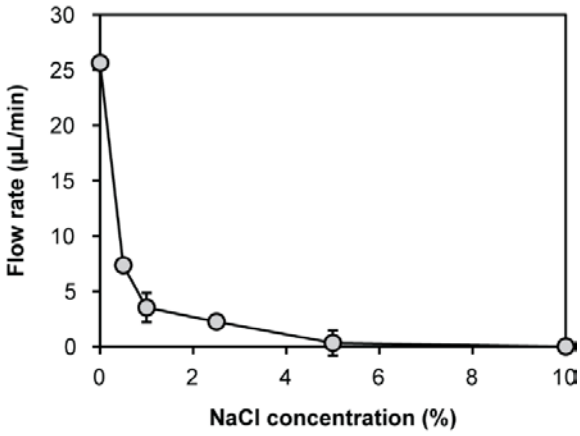

Figure 11. Dependence of the injection flow rate of DI water on the DI water and different concentrations of NaCl solutions added to the polymer disc. DI water used as a sample solution to be transported. (n = 3).

The extraction flow rates can be tuned by changing the composition and the different proportions of sodium polyacrylate (SP) and cellulose acetate (CA) in the polymer disc (Fig. 12): (i) ratio of SP and CA was 1:0.5, and prepared with DI water (ii) ratio of SP and CA was 1:1, and prepared with DI water (iii) ratio of SP and CA was 1:1.5, and prepared with DI water and (iv) ratio of SP and CA was 1:1.5, prepared with saline solution (0.9 % NaCl) or organic solvent (aq. ethanol) [11]. The lowest flow rate was obtained for the case of (iv) and the highest rate was attained for the cases (i) and (ii), but, the solution was split during extraction. The best result with an optimum flow rate was achieved for the case of (iii), in which all the solution was smoothly extracted from the reaction chamber.

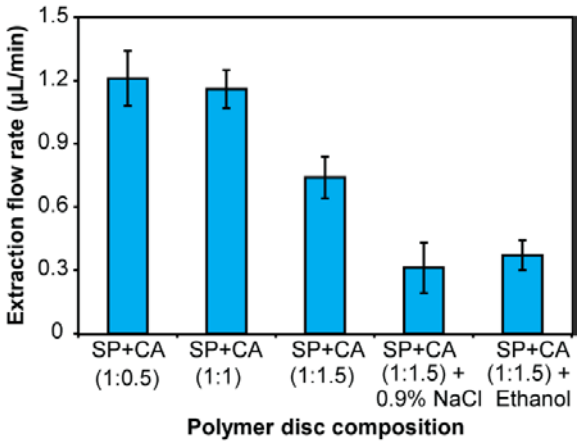

Figure 12. Dependence of the extraction pump efficiency on the different composition of the SP polymer disc. (n = 3).

Chapter 4: Control of microfluidic solution transport by switchable hydrophobic microvalves based on a conducting polymer

The chapter aims to develop a new valve that can be integrated into the integrated device for the exchange of solutions efficiently with minimal user intervention. In microfluidic devices, the integration of micropumps and microvalves is indispensable to carry out flow regulation in flow channel networks [11]. However, the integration of such elements into low-cost disposable analytical devices presents a challenge. To this end, microfluidic transport by capillary action and flow control by hydrophobic patch valves are realistic. The hydrophobic valves were used in combination with the application of pressure. A solution stopped at the valve passes through the region by the application of pressure [12]. However, with this method, a pressure source is required to realize the valve function. To solve this problem, our group has reported a switchable hydrophobic valve based on the switching of the mixed potential [13]. However, a problem with this valve was contamination by alkane thiol dissolved after opening the valve. In this study, we developed a valve using a conducting polymer polypyrrole (PPy). The valve consisted of a platinum electrode covered with a hydrophobic sodium dodecylbenzenesulfonate-doped polypyrrole (NaDBS-doped PPy) film. The hydrophobic PPy film takes hydrophobic and hydrophilic states upon the application of appropriate potentials to the platinum electrode [14]. Following this change, a solution stopped by the hydrophobic valve passes the valve region. The application of the valve was demonstrated in a microfluidic device.

To fabricate the valves, platinum (300-nm-thick) was deposited on a glass substrate by sputtering with a 50-nm-thick chromium intermediate layer. Electrode patterns were formed by lift-off. To deposit PPy, the platinum electrode was immersed into a solution containing 0.2 M pyrrole and 0.2 M NaDBS, and a constant current (1 mA/cm^2) was applied to the electrode for 120 s using a potentiostat (Autolab PGSTAT12; Eco Chemie, Utrecht, Netherlands). Finally, the surface was rinsed with ultra-pure water and dried by blowing N_2 gas.

The valve structure was made by bonding a poly(dimethylsiloxane) (PDMS) substrate with a flow channel structure and a glass substrate with a thin-film platinum electrode on which a surfactant sodium dodecylbenzenesulfonate-doped polypyrrole film (NaDBS-doped PPy) was formed (Fig. 13A). An inlet and an outlet were formed by punching a hole of 4 mm diameter (punch no. 1256, Takashiba Gimune Seisakujo, Hyogo, Japan) in the PDMS layer. To characterize the valve, a 0.1 M KCl solution was first injected into the solution inlet. The solution moved in the flow channel by capillary action, but stopped at the edge of the valve. A commercial Ag/AgCl reference electrode (2080 A-06T, Horiba, Kyoto, Japan) was then inserted into the solution inlet (Fig. 13A), and a potential was applied to the valve electrode using a potentiostat (HA-151, Hokuto Denko, Tokyo, Japan) with respect to the Ag/AgCl reference electrode. Fig. 13B explains the principle of valve operation. The application of a reductive potential to the platinum electrodes switched the valve from a hydrophobic state to a hydrophilic state via the reorientation of dopant molecules according to [(PPy^+)n DBS^-] + Na^+ + e^- ↔ [$(PPy^0)_n$ DBS^- Na^+] [14]. Following this, the solution started to pass through the valve region and moved forward in the flow channel.

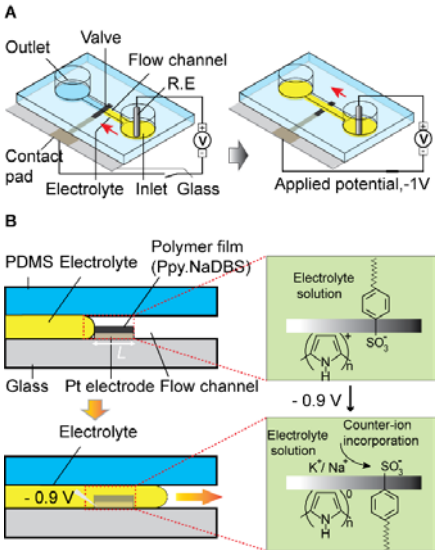

Figure 13. (A) Test device with a switchable hydrophobic valve formed in a flow channel. (B) Principle of operation.

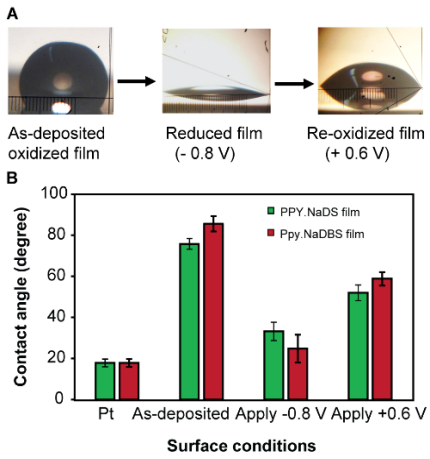

Figure 14. Change in wettability of the doped PPy by the application of potential. (A) Water-droplet on NaDBS-doped PPy coated Pt surfaces at as-deposited film, reduced film and re-oxidized film (B) Surface wettability behavior of the clean flat Pt surface, surfactant doped PPy coated Pt surface(native), reduced and re-oxidized surface of doped PPy coated Pt. (n=6).

To select an appropriate dopant (surfctant) for the valve, the wetting behavior of doped polypyrrole film was evaluated by measuring the water contact angle. Fig. 14B shows the contact angle of the PPy film when NaDBS and the other dopant, sodium dodecylsulphate (NaDS), were used. The change in the wettability of the PPy film could be enhanced by the addition of a dopant NaDBS as confirmed by contact angle measurement. The length of time for elcetropolymerization was also optimized based on the wettability measurement at each stages of switching cycle. When the polymerization time was longer than 60 s, the contact angle of the as-deposited film tended to saturate at 86 ± 1 degrees. However, the changes in wettability of the as-deposited, reduced, and re-oxidized films were larger for 120 s polymerization time than that of the other cases. Thus, the polymerization time was 120 s unless otherwise noted.

To demonstrate the flow control, a 100-µm long valve with a NaDBS-doped PPy layer was formed in a straight flow channel (500 µm wide) (Fig. 15A). A solution containing 0.1 M KCl was injected into the solution reservoir. The solution started to move by capillary action and was stopped at the valve edge. When −0.9 V was applied to the platinum electrode, the surface area of the valve that was in contact with the solution became more hydrophilic via reorientation

of the dopant molecules and the solution passed through the valve region. Once the solution reached the end of the valve, the solution flowed forward in the flow channel by capillary action. Without applying the potential, the valve could stop the solution stably for more than 10 min.

Then, switching time (time for the solution to cross the valve area after the application of the potential) was measured by forming valves of different lengths. Here, the length of the valve (*L*) indicates the length along the flow channel. Fig. 15B shows the switching time of the valves of different lengths. The switching time decreased with the decrease in valve length and was the shortest (5 s) with 50 µm long valves. The effect of applied potential on the switching time for 100-µm long valves is shown in the inset to Fig. 15B. When potential was more positive than −0.8 V, no influence was observed. However, the switching time decreased to 5 ± 1 s with potentials more negative than −0.8 V. The effect of solution pH on switching time was examined using a 100-µm long valve (Fig. 9). The switching time became longer in the pH range between 2 and 4, became almost steady for pH in the range between 5 and 9, and substantial decrease for the pH of 10. However, at the higher pH range between 11and 13, the valve did not function properly and the solution moved across the valve area without the application of the potential.

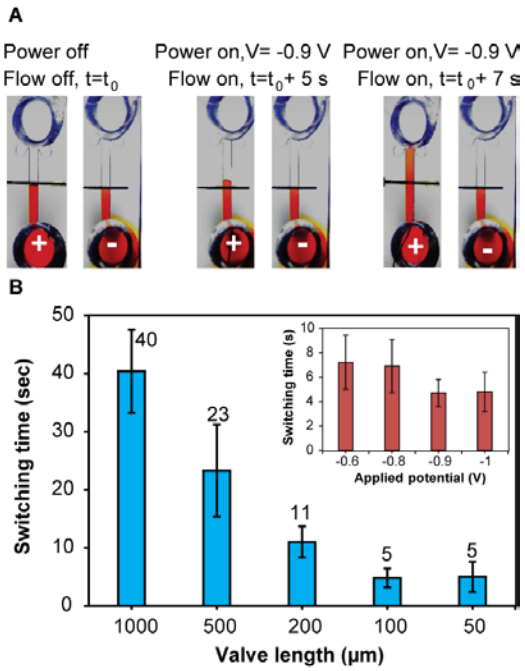

Figure 15. (A) Flow control using a 100-µm long valve. Flow channel width: 500 µm. Solution pH: 7.0. The same device structure was used for both cases. In the case of (+), −0.9 V was applied. On the other hand, no potential was applied in the case of (–). (B) Switching times with different lengths of the valve. (n=10). Inset: Dependence of switching time on applied potential. Valve length: 100 µm. Solution pH: 7.0 (n=10).

Also, the effect of the dopant concentration on the valve switching time was examined using the 100-µm long valves formed with NaDBS of different concentrations. When the concentration was higher than 0.2 M, the solution never stopped at the valve edge and passed over the valve without the application of potentials. On the other hand, the switching time was substantially reduced to 2 s and 1 s when the dopant concentration was 50 mM and 25 mM, respectively.

We also demonstrate selective transport of solutions using the valves. Fig. 17A shows a linear multiplexer. In this case, all six valves were controlled via the common contact pad. Initially, the potential was applied to open the valves that were in contact with solution, after that the switch was “off” and the switch was “on” again to open the subsequent valves. Fig. 17B shows a radial flow channel structure with eight-valves. In this case, the solution can be distributed selectively to the eight different microchannels from a reservoir at the center. Solutions loaded in the inlet is stopped at each valve (Fig. 17B (i)). Selected flow channels are opened by applying the potential (Fig. 17B (ii-iii)). Fig. 17C shows a device of a different layout with six-valves formed in a comb-shaped flow channel structure. By applying the potential, the solution penetrates into selected flow channels (Fig. 17C (ii-iii)). Additionally, the applicability of the valve was shown in a flow focusing device to enabling of hydrodynamic focusing in the main flow channel (Fig. 18).

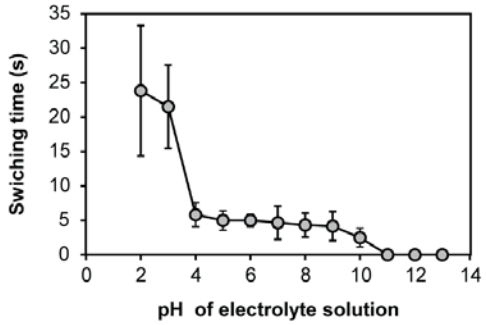

Figure 16. Dependence of switching time on the pH of the solution for a 100 µm valve (n=6).

Finally, the exchange of multiple solutions with minimum user intervention was performed using integrated device in which the valves were incorporated into the device as described in chapter 3 (Fig. 19).

Chapter 5: Summary

In this thesis, the development of microfluidic device with on-chip solutions exchange facility for immunoassaying is presented. The efficient solutions exchange in microfluidic device are demonstrated by the integration of SP polymer-based micropumps and polypyrrole-based valves. Hopefully, the developed device could be an effective tool for the POC measurement of protein biomarkers.

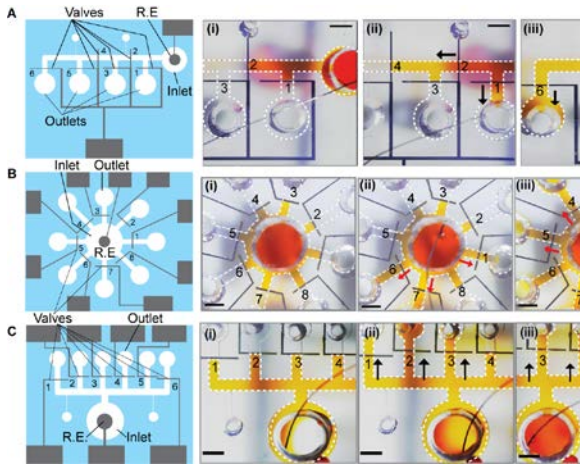

Figure 17. Multivalve operation in microfluidic system.(A) Linear multiplexer. (B) Radial multiplexer. (C) comb-shape multiplexer. To aid visualization, dye solution containing 0.1 M KCl, pH 7. Scale bar: 1 mm. R.E.: reference electrode, μC: microchannel.

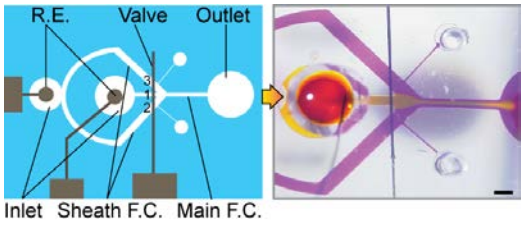

Figure 18. PDMS flow focusing device with NaDBS-doped PPy based microvalve. Hydrodynamic focusing state achieved by opening the valve upon the application of potential. Scale bar: 1 mm. F.C.: Flow channel.

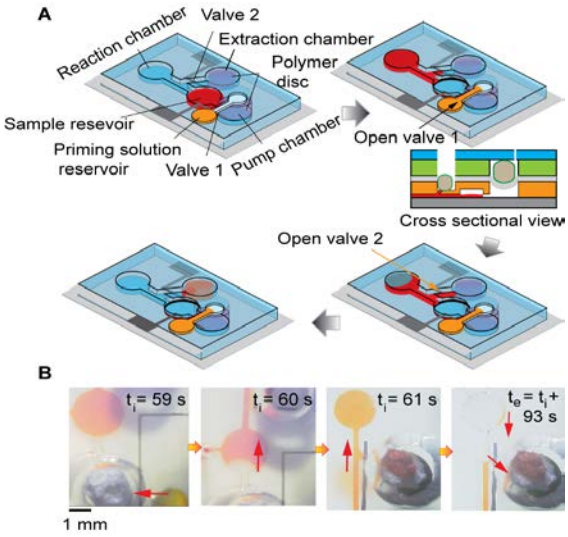

Figure 19. Exchange of solution on-chip with minimal user handling steps. (A) Principle of exchange of solution using the integrated device. (B) Images show that the exchange of solution using the device

References

1. Laxminarayan, R., Mills, A. J., Breman, J. G., Measham, A. R., Alleyne, G., Claeson, M., & Jamison, D. T., *The Lancet*, **2006**, 367(9517), 1193-1208.
2. Gubala, V., Harris, L. F., Ricco, A. J., Tan, M. X., & Williams, D. E., *Analytical chemistry*, **2011**, 84(2), 487-515.
3. Sanjay, S. T., Fu, G., Dou, M., Xu, F., Liu, R., Qi, H., & Li, X., *Analyst*, **2015**, 140(21), 7062-7081.
4. Whitesides, G. M., *Nature*, **2006**, 442(7101), 368.
5. Li, J.; Chang, K.-W.; Wang, C.-H.; Yang, C.-H.; Shiesh, S.-C.; Lee, G.-B., *Biosensors & Bioelectronics* **2016**, 79, 887 - 893.
6. Im, S. B.; Uddin, M. J.; Jin, G. J.; Shim, J. S., *Lab on Chip*, **2018**, in press.
7. Findlay, J. W. A., Smith, W. C., Lee, J. W., Nordblom, G. D., Das, I., DeSilva, B. S., & Bowsher, R. R., *Journal of pharmaceutical and biomedical analysis*, **2000**, 21(6), 1249-1273.
8. Squires, T. M., & Quake, S. R., *Reviews of modern physics*, **2005**, 77(3), 977.
9. Hu, Y., Beach, J., Raymer, J., & Gardner, M., *Journal of Exposure Science and Environmental Epidemiology*, **2004**, 14(5), 378.
10. Ogawa, I., Yamano, H., & Miyagawa, K., *Journal of applied polymer science*, **1993**, 47(2), 217-222
11. Au, A. K., Lai, H., Utela, B. R., & Folch, A., *Micromachines*, **2011**, 2(2), 179-220.
12. Handique, K., Burke, D. T., Mastrangelo, C. H., & Burns, M. A., *Analytical chemistry*, **2000,** 72(17), 4100-4109.
13. Biswas, G. C., Watanabe, T., Carlen, E. T., Yokokawa, M., & Suzuki, H., *ChemPhysChem*, **2016**, 17(6), 817-821.
14. Xu, L., Chen, W., Mulchandani, A., & Yan, Y., *Angewandte Chemie International Edition*, **2005**, 44(37), 6009-6012.